Bull. Pharm. Sci., Assiut University, Vol. 47, Issue 2, 2024, pp. 699-721.

Bulletin of Pharmaceutical Sciences
Assiut University
Website: http://bpsa.journals.ekb.eg/

BULL. PHARM. SCI. Assiut Univ.

DEVELOPMENT OF SERICIN HYDROGEL INCORPORATED WITH GREEN SYNTHESIZED CERIUM OXIDE NANOPARTICLES USING *SECURINEGA LEUCOPYRUS* FOR CHRONIC DIABETIC WOUND HEALING APPLICATIONS

k. Sriram * , G. Priyanka, TN. Dhanushri, A. udhayadharshini

Department of Biotechnology. Mepco Schlenk Engineering College, Sivakasi-626005, Tamil Nadu, India

Now a days the biomaterials made of sericin from waste Bombyx mori cocoon has created elevated interest among research community due to their high biocompatibility with wide range of cell lines. In our present study, we reported the synthesis of cerium oxide nanoparticles (CeONPs) from the plant extract of Securinega leucopyrus and incorporated in sericin hydrogel for the development of novel nanocomposite for wound healing applications. The plant extract acts as both reducing as well as stabilizing agent which helps in the conversion of cerium nitrate to cerium oxide. To analyze the properties of the synthesized nanoparticles various physiochemical characterizations such as UV-visible spectrophotometry, Dynamic Light Scattering (DLS), Scanning Electron Microscopy (SEM) and Transmission Electron Microscopy (TEM) were performed. UV-Visible spectrum of the synthesized nanoparticle showed distinct peak at 240 nm. The size and charge of the nanoparticle was investigated using DLS and was found to be 186.7 nm and -22.5 mV. The plant extract and the cerium oxide nanoparticles also showed antibacterial activities against gram-positive (Staphylococcus aureus) and gram-negative (Escherichia coli) microorganisms. The plant extract and the nanoparticles synthesized showed anti-oxidant activity with radical scavenging of 83.4 % and 76.48 % respectively. The hydrogel also exhibited good water retention property and swelling behavior. The drug release kinetics were studied for obtained sericin hydrogel. The plant extract and CeONPs loaded hydrogels also exhibited good antibacterial activity. Hence, our results conclude that sericin nanocomposite hydrogel could be the potential candidate in healing chronic wounds.

Keywords: *Chronic diabetic wounds; Securinega leucopyrus; Cerium oxide Nanoparticles; Sericin; Hydrogels*

INTRODUCTION

Diabetes is a chronic metabolic disease which is marked by high blood glucose levels. It affected over many individuals and especially it consumes most of the adult's annual health expenditure. In future, diabetes is projected to affect over 700 million individuals by 2045 [1,2]. Extended exposure to high levels of blood glucose induces certain effects and thereby suppresses the immune system and thus contributes to the impaired wound healing, prolonged inflammation, and reduced tissue epithelization kinetics. In diabetic patients, wounds are critical, difficult to heal and often prone to infection. These non-healing chronic diabetic wounds remain a challenge to the surgeon. These chronic wounds may lead to amputation if appropriate treatment is not provided to the patient[3]. There are many advances in modern surgical methods for these non-healing wounds, but management of these wounds remain critical. Ayurveda also provides various herbal formulations for chronic wounds, so many patients prefer ayurvedic formulations as their choice, but evidences of

Received : 2/5/2024 & Accepted : 13/8/2024

*Corresponding author: sriram k , E-mail: sriram@mepcoeng.ac.in

curing wounds for these formulations remain limited.

Impairment in healing diabetic wounds is a serious health challenge. Maintaining healthy glucose levels can avoid wounds and would heal faster [4]. There are approaches available for treating these non-healing wounds and are certain novel therapies and biological dressings. Wound healing is a natural physiological process due to structural damage of tissues. Healing of wounds occurs through four phases: hemostasis, inflammation, reepithelization (proliferation), remodeling (scar maturation) [5,6]. Various methods are available for treating the diabetic wounds which comprises of both modern and traditional methods. Current treatment strategies include cell-based therapies, biologically derived compounds-based therapy, certain physical methods and skin substitute based methods [7]. If these therapies do not contribute to heal the chronic wounds, amputation was the only choice of surgeons. Though, there are many advances developed in modern surgery, the management of these non-healing wounds is still complicated to the medical professionals. Traditionally, many medicinal plants and herbs have been proved with good wound healing efficiency. It helps in natural healing process by providing the requisite environment and it also involves disinfection, debridement. The compounds present in these medicinal plants are less toxic and also shows lesser side-effects than the modern medicines. The formulations from these plants are preferred for wound healing but with narrow evidences [8]. Medicinal plants contributed for healing chronic diabetic wounds are species of leucopyrus such as *Securinega leucopyrus, Flueggea leucopyrus*. The traditional strategies outweighed the modern methods in terms of side- effects .[9,10]

Hydrogels are 3D polymeric network, used successfully in various biomedical fields[11,12]. They act as an alternative for extracellular matrix (ECM) and thus help to create a moist environment which promotes the process of wound healing (hemostasis, inflammation, re-epithelization (proliferation), remodeling (scar maturation) [13, 14]. There are several methods for the fabrication of hydrogels, such as radiation and freeze-thaw processes. The freeze-thaw method is efficient as it does not require any toxic chemical compounds for the formation of hydrogels [15]. Different biopolymers such as sericin, chitosan, carboxymethyl chitosan (CMC), PVA were used in the synthesis of hydrogel wound dressings [16]. Nanoparticles are incorporated in the wound dressing in order to promote quick healing of chronic and acute wounds due to their antibacterial and anti-inflammatory properties.

Sericin is a natural protein extracted from *Bombyx mori (silk worms).* Sericin and fibroin together forms silk. While fibroin of the silk provides the structural integrity, sericin acts like a gum that holds the fibroins together [17, 18]. In silk extraction process, the sericin removed as a waste product. However, being a natural product sericin has good biocompatibility with most of the cell culture applications. Sodium alginate also has good biocompatibility and immunogenicity [19]. The combination of sericin with sodium alginate provides structural integrity to the hydrogel also provides support to the growth of new cell formation at wounded sites [20]. Hence, the biocompatible hydrogel infused with the antimicrobial CeO nanoparticles was considered as a good option of materials for the investigation of wound healing applications.

In this paper, we report for the first time a green and simple method for the preparation of CeONPs at room temperature using the *S. leucopyrus* extract as the reducing and stabilizing agent. We then incorporated these CeONPs into a sericin hydrogel. The hypothesis of this study is that the addition of CeONPs to sericin-gelatin nanocomposite hydrogel, will provide antibacterial properties against antibiotic resistant bacteria which will help in curing chronic wound. Further, physicochemical properties along with the antimicrobial activities of the hydrogels were analyzed to demonstrate their ability to serve as improved wound dressing materials in vitro. The results have also confirmed that the prepared CeONPs incorporated hydrogels were exhibited good antioxidant as well as antibacterial property which is important characteristic required for material applied for wound healing applications. Our experimental data supports our hypothesis of novel nanoparticles incorporated hybrid hydrogel has the potential application in the treatment of chronic wound.

MATERIALS AND METHODS

Materials

Securinega leucopyrus plant powder was obtained from Ayu Medicines, Gujarat, India. Solvents such as methanol and acetone purchased from Loba Chemie, Mumbai, India. Cerium nitrate, sodium hydroxide, DPPH (2,2-diphenyl-1-picrylhydrazyl) and sodium carbonate were purchased from Merck, Mumbai, India. sodium alginate and calcium chloride were purchased from Sigma Aldrich, Mumbai, India. All reagents used were of analytical grade and were used without any further purification. Millipore water was used for all preparation steps to avoid contamination. The bacterial strains used for the antibacterial assays were *Staphylococcus aureus* and *Escherichia coli* Dh5α. The mediums such as Luria broth, Luria agar, nutrient broth and nutrient medium were purchased from HiMedia Laboratories, Mumbai, India. The mulberry silk cocoons were bought from a local sericulture farm at Tenkasi, India.

Methods

Preparation of *Securinega leucopyrus* plant extract

Plant extracts were prepared with different solvents such as water, acetone, and methanol. Acetone and methanol extracts were prepared using the Soxhlet apparatus (at 70 ºC). For the preparation of water extract, *S. leucopyrus* powder (1.33 g) was boiled in 100 ml distilled water for 30 mins. The extract was filtered using Whatman filter No.3 [21]. The extracts were stored and were further analyzed for various bio-active compounds through GC-MS (Gas Chromatography-Mass Spectroscopy) analysis. These compounds were screened based on its properties towards wound healing. Researchers mentioned that the matrix metalloproteinases 8 (MMP-8) and matrix metalloproteinases 9 (MMP-9) act as specific targets for chronic diabetic wounds which are only present in diabetic patients. Moreover, the dysregulation of MMPs may lead to prolonged inflammation and delayed wound healing. These compounds were further screened for its drug-like properties through Lipinski's rule of five [22]. The interaction between these bioactive compounds identified and the targets, MMP-8 and MMP-9 were observed through PyRx and PyMol softwares [23].

Synthesis of CeONPs

The synthesis of CeONPs nanoparticles is referred from Mamatha et al, 2024 [24] with some minor modification. Different concentrations of cerium nitrate solutions (5 mM, 10 mM, 15 mM) were prepared. 1 ml of 5 mM cerium nitrate, 1 ml of *Securinega leucopyrus* plant extract and 7 ml of milli-Q water was mixed at room temperature (28 ºC) and 1 ml of 30 mM NaOH was added dropwise to the mixture to obtain 10 ml CeONP suspension. The suspension was sonicated at 75 % amplitude with 59/10 seconds on/off pulse for complete dispersion. The suspension was filtered and centrifuged at 6000 rpm for 15 mins. The protocol was performed for each concentration of cerium nitrate and plant extract with different solvents. The CeONP prepared in the water solvent was used to load inside the hydrogel**.**

Characterization of synthesized nanoparticles

Light absorption property for plant extract with different solvents and cerium nitrate solution of different concentrations was checked by a spectrophotometer in the wavelength region 200-800 nm using UV-vis Spectra (model: Halo-DB-20 double beam UV-VIS Spectrophotometer, HITACHI, Japan). Similarly, the spectra were recorded for the prepared CeONPs suspensions with different concentrations in the same wavelength region. The results were recorded.

Dynamic Light Scattering was performed to identify the hydrodynamic size distribution and zeta potential (stability in reference to surface charge) of the synthesized CeONPs suspensions using a Nano ZS zetasizer system (Malvern Instruments), UK. Measurement parameters were: measurement temperature of 25 °C, material refractive index of 1.59, dispersant refractive index and viscosity of 1.330 and 0.8827 cP respectively.

The shape, morphology, and dispersal characteristics of the nanoparticles were analyzed by Scanning Electron Microscopy (SEM) TESCAN VEGA3 SBH Czech Republic. The shape, morphology, and dispersal characteristics of the nanoparticles were analyzed by an SEM microscope.

Size, shape and internal features of the NPs were determined by Transmission Electron Microscope (TEM) FEI Tecnai G220 S-TWIN TEM, USA; 1 mg of CeONP powder was

placed in a grid, in a vacuum desiccator and was finally analyzed by TEM, operated at 200 kV.

The IR spectra of pure drug and hydrogel loaded with drug was obtained by Fourier Transform Infrared Spectroscopy, Nicolet Avatar 330 FTIR, Thermo Scientific, United States of America technique to test drug-polymer interaction and the stability of drug loaded.

Antibacterial activity of CeONP against both gram-positive (*Staphylococcus aureus*) and gram-negative bacteria (*E. coli*), which are the most common wound-infecting microorganisms. The antimicrobial activity of the NPs was tested based on the well agar diffusion method. 100 µl of a suspension of bacteria were first uniformly coated on the LB media. After drying the plates, the wells were punched and the samples were loaded. Ampicillin was used as the positive control and the inhibitory zones of the drug and the nanoparticle synthesized was evaluated.

Antioxidant activity of CeONP was determined by the DPPH (2-diphenyl-1-picrylhydrazyl) assay. DPPH was composed of stable free radical molecules and its purple-coloured solution had a strong absorption peak at 517 nm. When its radical property was scavenged upon absorption of hydrogen from an antioxidant, the colour turned from purple to yellow with decrease of intensity of (abs) 517 nm. The antioxidant activity was calculated by Eq (1):

$$\% \text{ Radial scavenging} = \frac{[(\text{DPPH})517\text{nm} - (\text{DPPH} + \text{antioxidant})517\text{nm}}{[(\text{DPPH})517\text{nm}]} \times 100 \quad (1)$$

Extraction of Sericin from silk cocoons

50 g of silk cocoons were chopped into pieces and washed in distilled water. Then it was immersed in water and the solution was autoclaved at at 121 °C and 15 psi pressure. The autoclaved solution was filtered to remove the insoluble compounds. The resultant solution was freeze-dried by lyophilization to obtain the powdered form of sericin and used for various characterizations [25]. The resultant solution was also used directly to form hydrogels.

Characterization of extracted sericin

Light absorption property of sericin extracted with water was checked by a spectrophotometer in the wavelength region 200-800 nm using UV-Visible Spectrometer.

Bradford assay was used for protein quantification, where bovine serum albumin (BSA) was used as a standard protein. Different aliquots of BSA were added to the solution of Coomassie Brilliant Blue G-250 and incubated at room temperature for 5 min and then the absorbance was measured at 595 nm. The standard graph was plotted with the absorbance obtained. Simultaneously, the sericin was added to the Coomassie Brilliant Blue G-250 solution and then incubated for 5 min at room temperature. The absorbance of the extracted sericin was measured at 595 nm [26]. The concentration of the sericin extracted was obtained by extrapolating the absorbance of the sericin solution obtained from the standard graph.

The thermal characterization of sericin extracted was accomplished through calorimetric assays. The sample was subjected to a linear temperature increase from 20 °C up to 400 °C, at a constant heating rate. The rate of degradation of the sample extracted was recorded and compared with the rate of degradation of the reference sericin extracted in previous literature studies.

The molar mass distribution of the extracted was investigated by sodium dodecyl sulfate polyacrylamide gel electrophoresis (SDS-PAGE) system from Bio-RAD. The molecular weight of sericin extracted was determined by 10 µl of the sericin extract was added to 10 µl of sample solubilizing buffer in an Eppendorf and then boiled for 10 min. Then, the SDS-PAGE analysis of sample (17 µl) and a protein standard ladder ranging from 10 kDa to 400 kDa was performed, with the gel run at a voltage of 100 V, 20 mA [27]. After the gel run, the gel was stained and then destained. Following destaining, the gel was documented for analysis.

Fabrication of hydrogel

Different concentration of sodium alginate (2 %, 4 %, 6 %, 8 % and 10 %) solutions were prepared using sericin solution extracted through autoclave method. 500 µl of the aqueous plant extract was loaded in 2 ml of sericin-alginate mixture of each concentration. Calcium chloride was used as the cross-linker, where 1.5% $Cacl_2$ was added to different concentration and the gel formation was observed. Similarly, the concentration of cross-

linker was varied over a range (0.25 %, 0.5 %, 0.75 %, 1 %, 1.25 % and 1.5 %). Then, 500 µl of aqueous plant extract was added to 10 % sericin-alginate mixture along with different concentrations of cross-linker. The gel formation was noted and the amount of drug loaded and unloaded was identified.

Properties of hydrogel

Water retention property

The dry hydrogel was immersed inside the phosphate buffer for 90 mins and then water retention property of the swelled hydrogel was evaluated by drying the gels in a hot-air oven at the temperature range of 37 °C. The weight change was noted at different time intervals [28]. The water retention activity of the hydrogel was calculated using the following Eq (2) and recorded.

$$\text{Water retention capacity (\%)} = \frac{Wt - WI}{WI} \times 100 \quad (2)$$

Where, W_I is the weight of the hydrogel at time 't', and W_I is the dried weight of the hydrogel before subjected to swelling.

Swelling behavior

The swelling behavior of the fabricated hydrogels was evaluated by immersing the fabricated hydrogels in phosphate buffer of different pH at room temperature and weighed at different time intervals [29]. The swelling capacity was calculated using the following Eq (3).

$$\text{Swelling (\%)} = \frac{WS - WD}{WD} \times 100 \quad (3)$$

Where, W_S is the swollen weight of the hydrogel, and W_D is the dry weight of the hydrogel.

Drug release kinetics

The CeONP aqueous plant extract of *S. leucopyrus* was prepared at different concentration and the absorbance was noted at 530 nm and a standard calibration curve was plotted. The release of plant extract with CeONP was observed by immersing the hydrogels in phosphate buffer at pH 7.4 and stirred (low rpm) at room temperature [30]. The absorbance of the release medium was measured at different time intervals and the cumulative drug release was calculated.

Antibacterial activity of hydrogels

Antibacterial activity of hydrogel against both gram-positive (*Staphylococcus aureus*) and gram-negative bacteria (*E. coli*), which are the most common wound-infecting microorganisms. The antimicrobial activity of the hydrogel was tested based on the well agar diffusion method [31]. A 100 µl of a suspension of bacteria were first uniformly coated on the LB media. After drying the plates, the wells were punched and the samples were loaded. Ampicillin was used as the positive control and the inhibitory zones of the drug and the nanoparticles synthesized was evaluated.

RESULTS AND DISCUSSION

Results

***Securinega leucopyrus* plant extract**

The *Securinega leucopyrus* plant powder was used to prepare extract solutions using different solvents (water, methanol and acetone). Different bio-active compounds were identified with wound healing, cell proliferation, tissue regeneration properties from the results of GC-MS analysis [32]. The peaks obtained is shown in **(Fig. 1)**. These bioactive compounds were further screened for its drug-like properties using Lipinski's rule of five such that 26 compounds were identified to have drug-like properties [33]. The interaction between these compounds and the targets, MMP-8 and MMP-9 were observed and shown in **(Table 1)**. It was also found that 2,4,7,14-Tetramethyl-4-vinyl-tricyclo [5.4.3.0(1,8)] tetradecan-6-ol (acetone), 6-Trifluoromethyl-benzo[4,5]imidazo[1,2-c]quinazoline (methanol) and Indolizine, 2-(4-methylphenyl)- exhibited a lower binding affinity of (-14.3, -13.5), (-10, -9.2) and (-8.2, 8.8) with MMP-8 and MMP-9 respectively, such that it possesses higher binding energy compared to other compounds identified and screened.

Table 1: Docking results of bioactive compounds identified and screened with MMP-8 and MMP-9.

Solvent	Name of compound	Binding affinity on interaction with MMP-8	Binding affinity on interaction with MMP-9
Acetone	2-(1-Phenylethyl)phenol	-7.2	-7.5
Acetone	Azulene, 1,4-dimethyl-7-(1-methylethyl)-	-7.0	-7.7
Acetone	Ergosta-5,7-dien-3-ol, (3.beta.)-	-8.8	-7.6
Acetone	2,4,7,14-Tetramethyl-4-vinyl tricyclo [5.4.3.0(1,8)] tetradecan-6-ol	-14.3 (a)	-13.5
Acetone	Curan-17-oic acid, 2,16-didehydro-20-hydroxy-19-oxo-, methyl ester	-7.1	-8.0
Acetone	D-Homoandrostane, (5.alpha.,13.alpha.)-	-8.2	-8.5
Acetone	Ergost-22-en-3-ol, (3.alpha.,5.beta.,22E)-	-8.3	-8.3
Acetone	gamma.-Sitosterol	-8.1	-8.0
Acetone	beta.-Sitosterol	-7.9	-8.1
Acetone	Xanthen-9-one, 1-hydroxy-3,5,8-trimethoxy	-7.9	-7.6
Acetone	5,5',8,8'-Tetrahydroxy-3,3'-dimethyl-2,2'-binaphthalene-1,1',4,4'-tetrone	-7.9	-9.6
Acetone	Tetradecanoic acid	-6.4	-4.7
Methanol	2-(1-Phenylethyl)phenol	-7.7	-6.8
Methanol	N,N-Dimethyldodecanamide	-5.8 (c)	-5.4
Methanol	1-Hydroxy-3,7,8-trimethoxyxanthene-9-one	-7.2 (b)	-7.5
Methanol	6-Trifluoromethyl-benzo[4,5]imidazo[1,2-c]quinazoline	-8.2	-8.8
Methanol	Morphinan-2,6-diol, 4,5-epoxy-N-methy-,(2.beta., 5.alpha., 6.alpha.)	-6.9	-8.3
Methanol	Xanthene-9-one,1-hydroxy-3,5,8-trimethoxy	-7.7	-7.5
Methanol	Methyl 2-[1-(4-methylphenyl)hydrazine]propanoate	-7.6	-6.3
Methanol	Acetic acid, [4-(1,1-dimethylethyl)phenoxy]-,methyl ester	-7.5	-6.0
Methanol	Acetamide, N-(4-fluorophenyl)-2,2,2-trifluoro	-8.0	-7.7
Methanol	2,4-Cyclohexadien-1-one, 3,5-bis(1,1-dimethylethyl)-4-hydroxy	-5.4	-6.8
Water	Indolizine, 2-(4-methylphenyl)-	-10.0	-9.2
Water	Cyclopentaneethanol, 2-(hydroxymethyl)-.beta.,3- dimethyl	-6.1	-5.7
Water	Benzo[h]quinoline, 2,4-dimethyl-	-9.4	-5.6
Water	1,2-Benzenediol, 3,5-bis(1,1-dimethylethyl)-	-6.2	-7.1

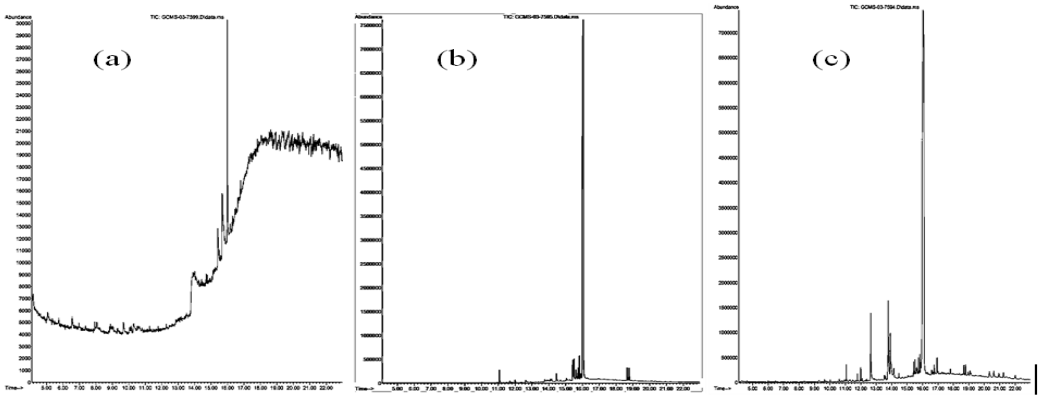

Fig. 1: Peaks obtained for different bioactive compounds present in the plant extracts extracted using (a) water (b) methanol and (c) acetone from.

Synthesis and characterization of CeONPs with *S. leucopyrus* aqueous extract

The aqueous extracts of *S. leucopyrus* plant powder was added to 10mM Ce $(NO_3)_3$ and 30 mM NaOH, cerium oxide nanoparticles were rapidly synthesized. The pH of the nanoparticle suspension before adding NaOH was recorded as pH 4.22 which then increased to 8.22 on addition of NaOH, due to the formation of cerium hydroxide. After 48 h of reaction, the pH of the nanoparticle suspension got reduced to 7.41. These results determined that the plant extract has the ability to reduce cerium nitrate to cerium oxide and bio-synthesize cerium oxide nanoparticles.

The UV-Vis absorption spectrum of the plant extracts obtained using water, acetone and methanol solvents showed a distinct peak at around 530 nm, 530 nm, and 660 nm respectively. Similarly, the absorption spectra peak of different salt solutions was around 220 nm and 230 nm for range of concentrations between 5 mM and 15 mM. The absorption peak of the nanoparticle suspension was around 240 nm. On comparing with peaks of extracts, salt solutions and the nanoparticle suspension, the nature of the spectrum indicates the presence of certain particles in the suspension. Therefore, the results of UV-Visible spectroscopic analysis shown in **(Fig. 2)** indicate the formation of the cerium oxide nanoparticles [34].

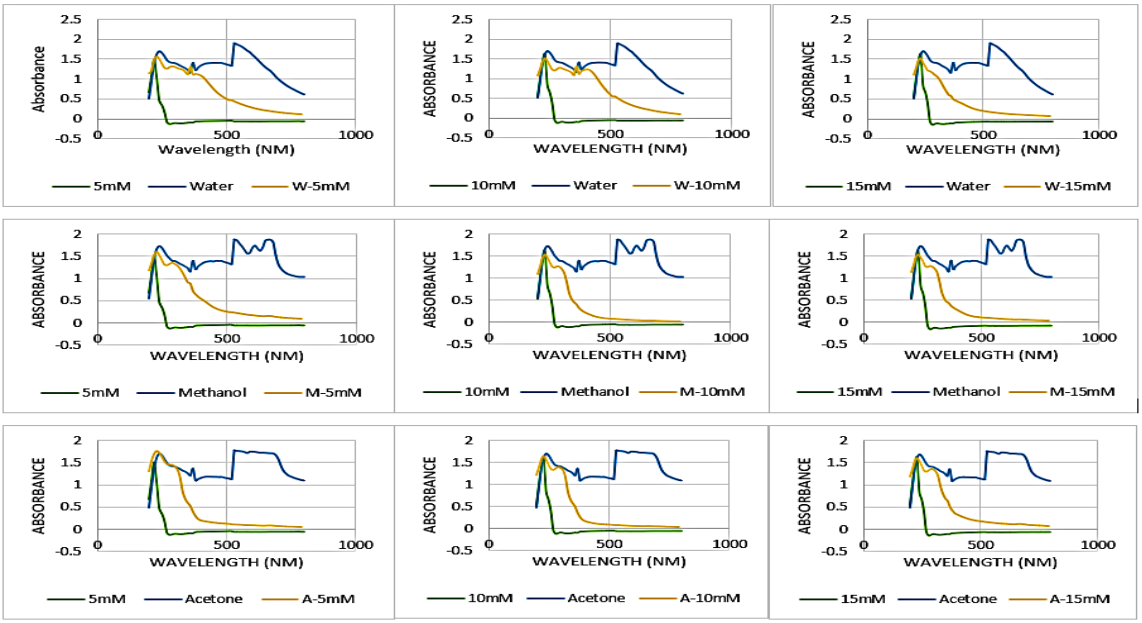

Fig. 2: UV-Visible absorbance peaks of water (a) methanol (b) and acetone (c) extracts, salt solutions and nanoparticle suspensions.

Different concentration nanoparticle suspensions were prepared and were subjected to DLS analysis and the zeta potential value, size of the nanoparticles and its poly dispersity were recorded as in (**Table 2)**. Among the suspensions, the zeta potential value for 10 mM CeONPs prepared using aqueous extract was obtained as -22.5 mV, which has higher magnitude

compared with other nanoparticle suspensions. This indicates that the synthesized cerium oxide nanoparticles were stable and well-dispersed as shown in **(Fig. 3).** However, the negative zeta potential value may be due to the capping agents which consist of negatively charged groups on the surface of the nanoparticles synthesized [35]. The 10 mM cerium oxide nanoparticles prepared using aqueous plant extract had a less particle size of 186.69 nm and a low poly-dispersity index of 0.163 compared with other CeoNP suspensions.

The SEM analysis of the synthesized nanoparticles showed spherical nanoparticles as shown in (**Fig. 4)**. The well dispersed particles in the size range of 100-200 nm are visible in the SEM analysis. To study the internal details of the individual particles TEM analysis performed along with SEM analysis [36].

The TEM micrographs of the synthesized cerium oxide nanoparticles showed that the sizes were between 50 nm and 200 nm. The size of the nanoparticle measured through zetasizer analyzer also matched with the size range provided by TEM analysis (**Fig. 5).**

Table 2: Size, poly dispersity index and zeta potential values of different CeONP suspensions from dynamic light scattering.

Solvents used to prepare CeONP solution	**Z-average (nm)**	**PDI**	**Charge (mV)**
5 mM-Acetone	27895.07	0.447	-8.63
10 mM-Acetone	8959.56	1	-2.54
15 mM-Acetone	6130.14	0.922	-0.081
5 mM-Methanol	729.79	0.49	-22.5
10 mM-Methanol	7198.23	0.957	-4.23
15 mM-Methanol	10951.35	0.565	0.339
5 mM-Water	278.98	0.248	-20.4
10 mM-Water	186.69	0.163	-22.2
15 mM-Water	2153.83	0.522	-12.2

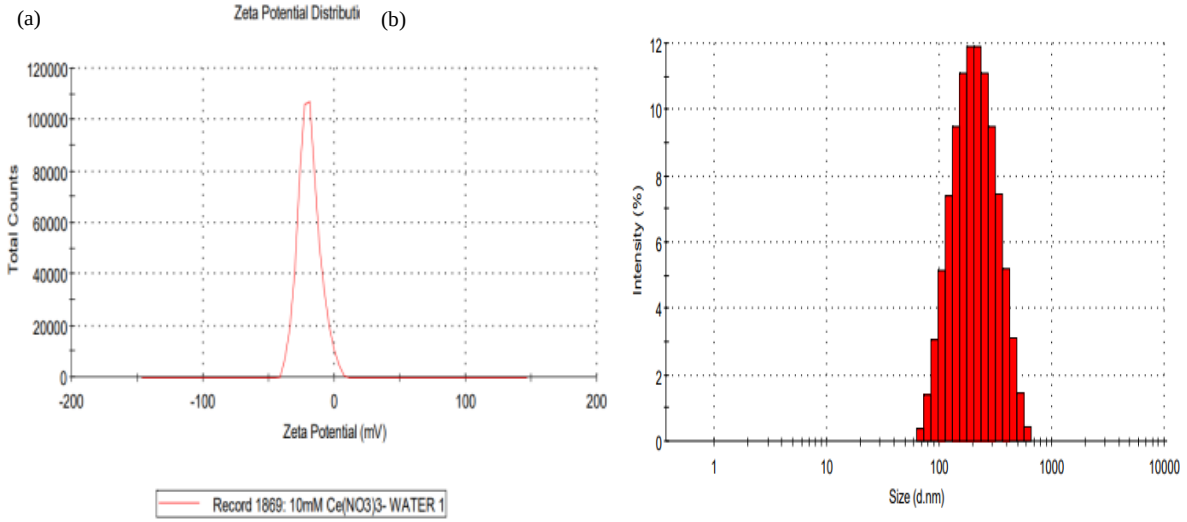

Fig. 3: Zeta potential (a) and Size distribution (b) of synthesized cerium oxide nanoparticles from dynamic light sacttering.

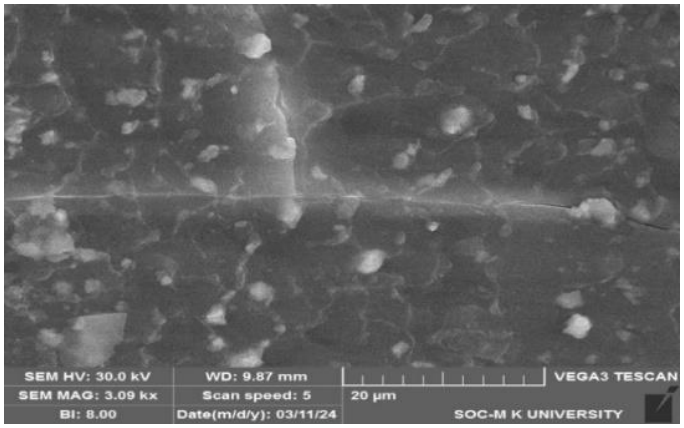

Fig. 4: SEM image of cerium oxide nanoparticles.

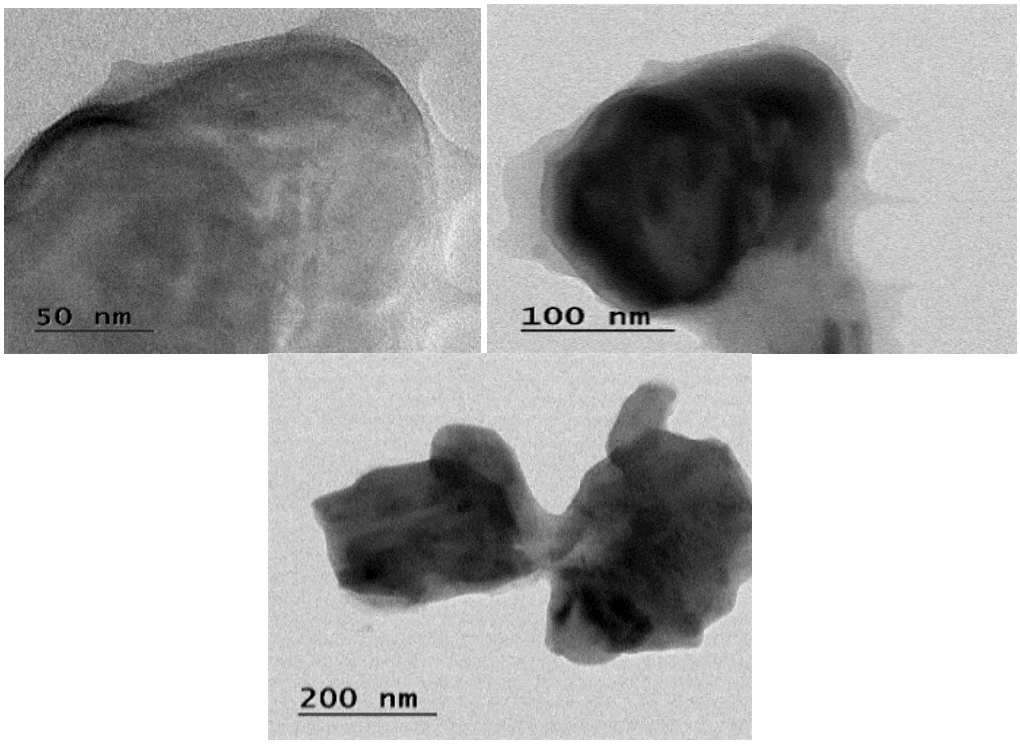

Fig. 5: TEM images of synthesized cerium oxide nanoparticles.

The antibacterial activity of the synthesized CeONPs were evaluated by testing a gram-positive bacterial strain and a gran-negative bacterial strain. **Fig.6** showed that on increasing the concentration of the aqueous extract of *S. leucopyrus* from 1 mg/ml to 100 mg/ml (1 mg/ml, 20 mg/ml, 40 mg/ml, 60 mg ml, 80 mg/ml and 100 mg/ml), the zone of inhibition produced against the strains also increased. For 100 mg/ml plant extract, the zone of inhibition was 8 mm and 7 mm against *S. aureus* and *E. coli* respectively. Therefore, 100 mg/ml aqueous extract produced higher zone of inhibition compared to other aqueous plant extract concentrations as in (**Table 3).** Similarly, the CeONPs antibacterial activity was also evaluated by testing both the strains. The concentration of the nanoparticles was also varied over a range of concentrations and the zones of inhibitions were reported. The zones of inhibition are shown in (**Fig.7)** and (**Table 4)**. Moreover, the zone of inhibition results revealed that Gram-positive bacteria was susceptible to the plant extract and the synthesized CeONPs compared with the Gram-negative bacteria. Gram-negative bacteria did not show any effect towards the aqueous plant extract of *S. leucopyrus* and the nanoparticles synthesized.

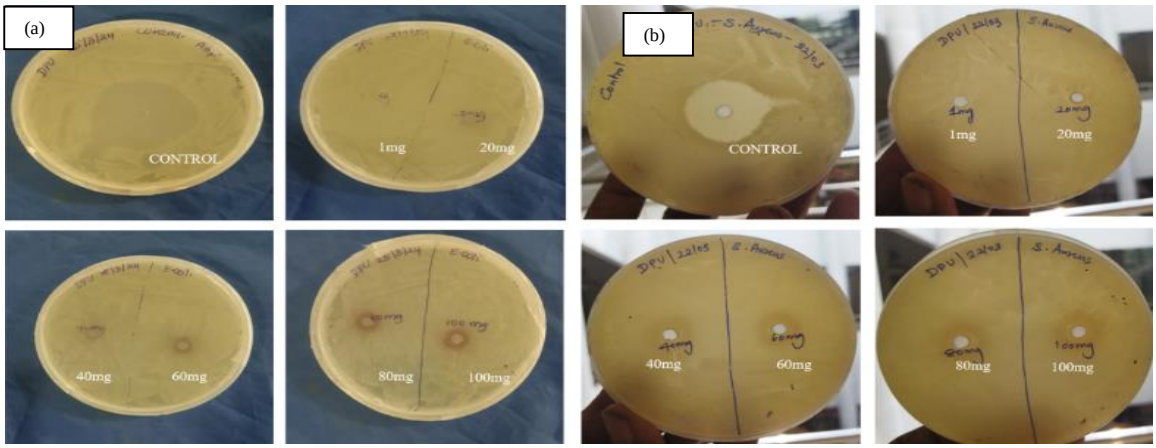

Fig. 6: Activity of aqueous plant extract of *Securinega leucopyrus* depicting the zones of inhibition against the selected microorganisms, *Escherichia coli* (A) and *Staphylococcus aureus* (B).

Table 3: Antibacterial activity assays of aqueous plant extract *Securinega leucopyrus* using agar well diffusion method.

Name of the organism	Concentration of aqueous plant extract (mg/ml)	Inhibition zones (mm)
Escherichia coli	Control (Amp^r)	25
	1	-
	20	-
	40	2
	60	3
	80	4.5
	100	5
Staphylococcus aureus	Control (Amp^r)	20
	1	-
	20	-
	40	6
	60	7.5
	80	8
	100	10

"–" no inhibition zone.

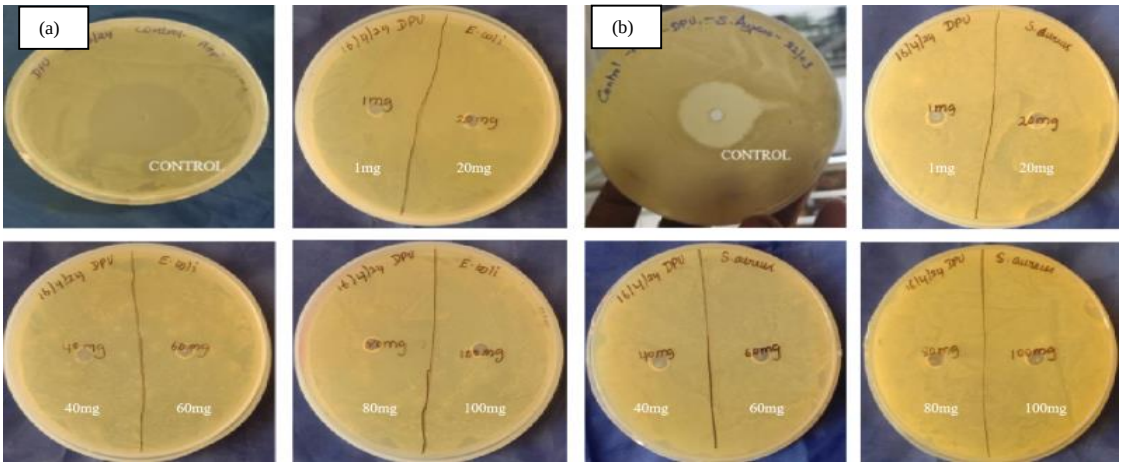

Fig.7: Activity of nanoparticle synthesized from aqueous plant extract of *Securinega leucopyrus* depicting the zones of inhibition against the selected microorganisms, *Escherichia coli* (a) and *Staphylococcus aureus* (a).

Table 4: Antibacterial activity assays of nanoparticles synthesized from aqueous plant extract *Securinega leucopyrus* using agar well diffusion method.

Name of the organism	Concentration of nanoparticle (mg/ml)	Inhibition zones (mm)
Escherichia coli	Control (Amp^r)	25
	1	-
	20	-
	40	-
	60	-
	80	-
	100	-
Staphylococcus aureus	Control (Amp^r)	20
	1	-
	20	-
	40	-
	60	5
	80	6.5
	100	7

"–" no inhibition zone.

The antioxidant property of the *Securinega leucopyrus* aqueous plant extract and the nanoparticles synthesized from the plant extract is evaluated using DPPH as substrate as shown in (**Fig. 8 (a-c)).** The antioxidant activity of the plant extract was observed to increase with increasing concentrations of the plant extracts. The standard antioxidant, ascorbic acid, showed good radical scavenging activity of 73.63% when tested with 1mg/ml. However, 1mg/ml aqueous plant extract, the radical scavenging activity was obtained to be 83.4% and 0.4 mg/ml CeONP suspension produced a radical scavenging activity of 76.48%. Therefore, the antioxidant activity of the aqueous plant extract was more compared to the antioxidant activity of the standard antioxidant**.** Similarly, the anti-oxidant activity of the nanoparticles was also more than the standard antioxidant.

Characterization of extracted sericin

The UV-Vis absorption spectrum of the sericin extracted using water showed a distinct peak at around 240 nm **(Fig.9 (a))** which indicates the presence of sericin protein in the extract. Similar studies have reported that a characteristic peak for sericin was obtained between 210nm and 280nm [37].

The sericin protein was estimated by the Bradford assay (). A standard calibration curve was plotted for protein using solutions of bovine serum albumin (BSA) in ddH_2O at several concentrations in the range of 0-0.05 mg/ml as in **Fig. 9 (b)**. This colorimetric method was used for protein quantification, the sericin extracted from water exhibited a protein concentration of 0.026 mg/ml.

The result of DSC analysis of sericin extracted was performed under the heating mode between 20°C and 400°C, shown in (**Fig.10)**. An endothermic peak was observed at 157.23°C. This endothermic peak may be due the evaporation of bound water molecules in the sample. The sericin denaturation had a n endothermic peak mainly observed at temperature 220°C.[38]

The results of SDS-PAGE analysis of the sericin solution **(Fig.11).** The lane 1 shows the wide range molecular weight markers ranging from 10 kDa to 170 kDa. The sericin extracted through autoclave method of extraction loaded in the lane 2 has shown broad range of molecular weight in the SDS-PAGE analysis. As cocoons were exposed to higher temperature for the sericin extraction, the peptide bonds of the primary structure of the protein gets attacked. Thus, broader bands are observed in lane 2 due to the mixture of different molecular weight peptides. Similar results were published by[39].

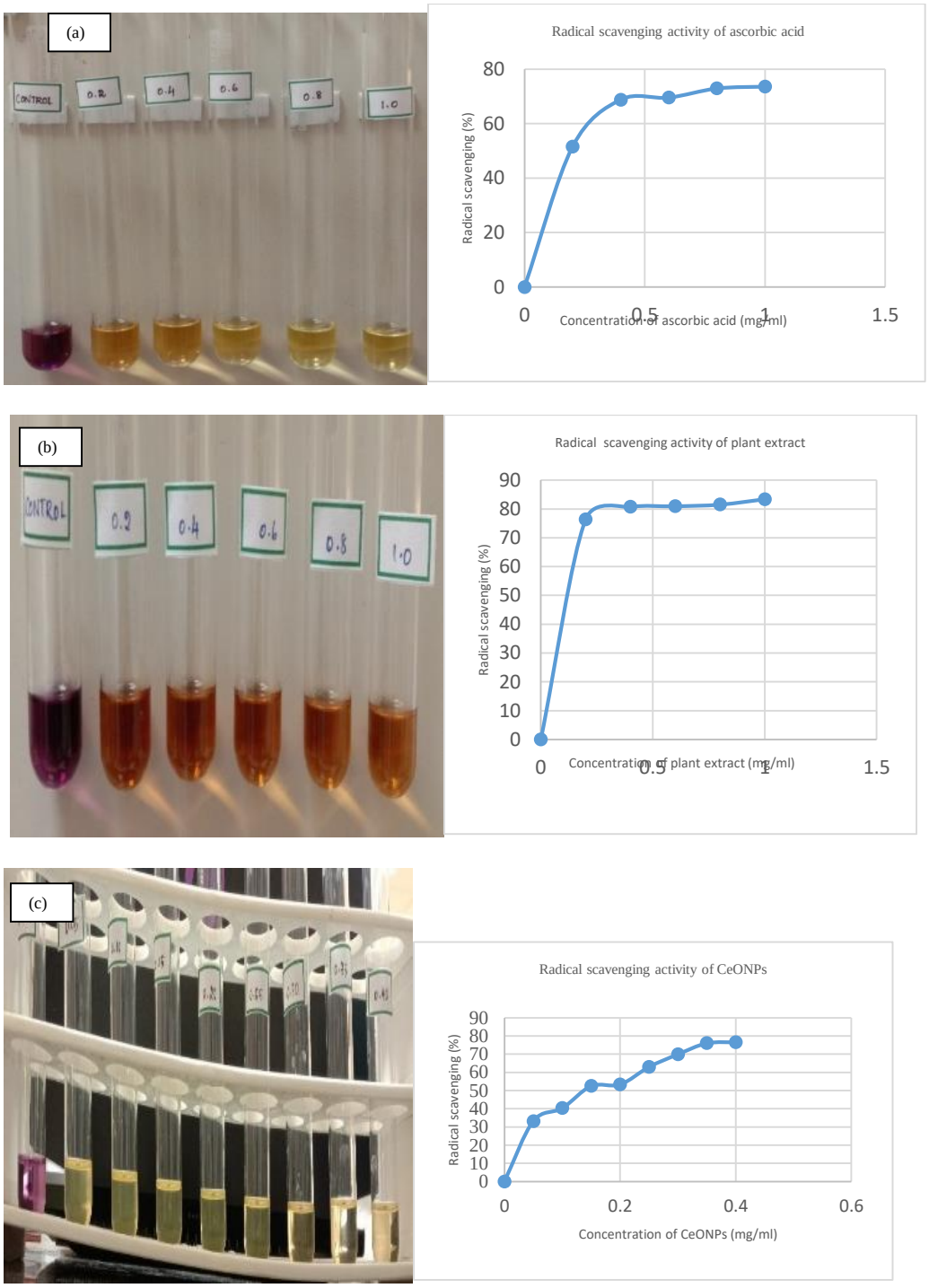

Fig. 8: DPPH radical scavenging activities of standard, Ascorbic acid (a), aqueous plant extract of *S. leucopyrus* (b) and nanoparticle synthesized using aqueous plant extract of *S. leucopyrus* (c) and the corresponding graphs.

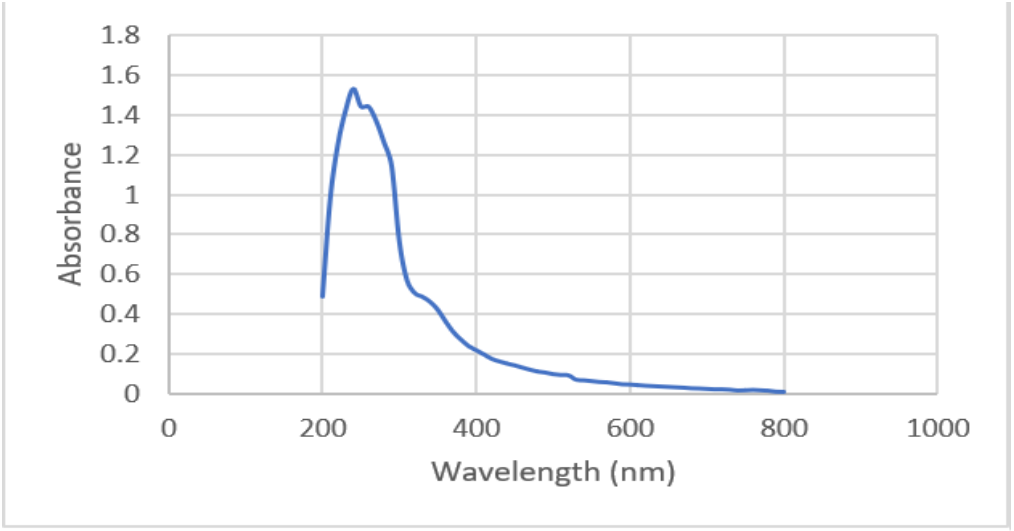

Fig. 9 (a): UV-Visible absorbance peaks of sericin extracted from water.

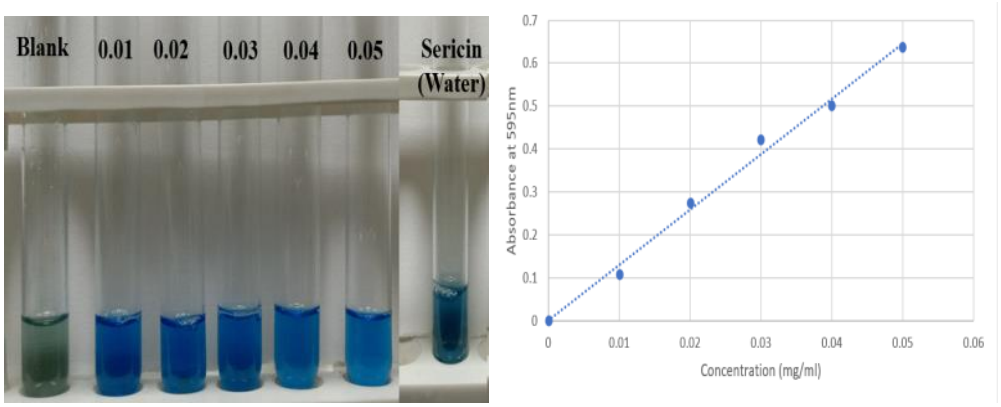

Fig. 9 (b): Estimation of protein (sericin) content through Bradford assay.

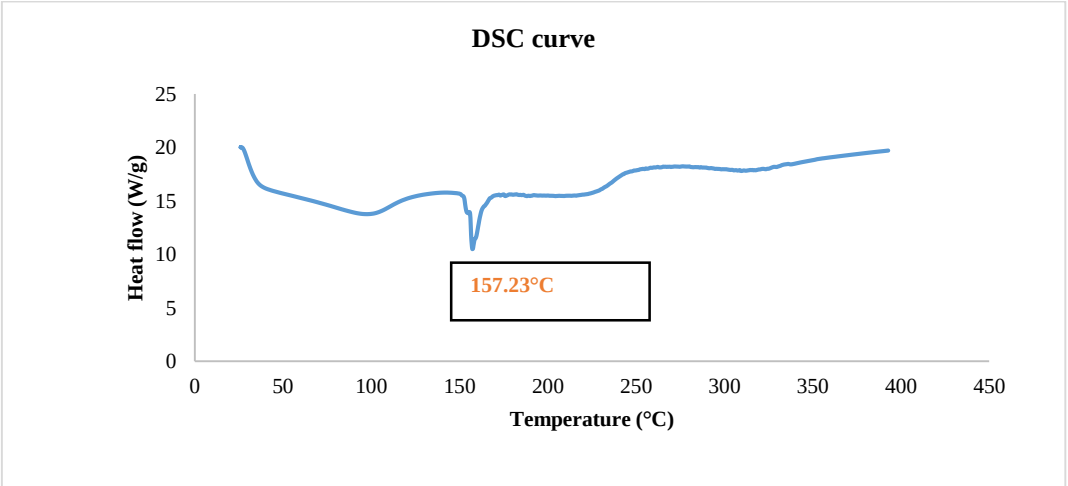

Fig. 10: DSC of silk sericin extracted by autoclave extraction method.

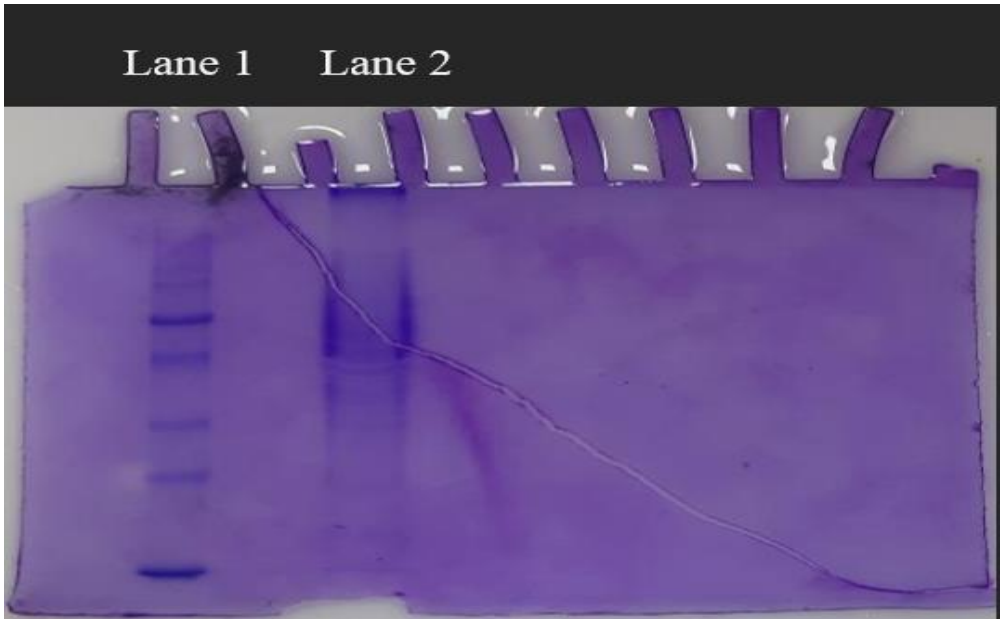

Fig. 11: Sericin protein estimation by SDS-PAGE.

Fabrication of hydrogel

The hydrogels were fabricated with different concentrations of sodium alginate and calcium chloride along with the 14.6 % sericine solution from silk cocoon. The sericine hydrogel formed with 1.5 % calcium chloride, 10% sodium alginate has rapid solidification capacity and the drug was completely loaded whereas, in other concentration the gel formation was too slow and drug was not completely loaded. Hence, this composition was used to prepare aqueous plant extract loaded sericin hydrogel and used for further studies.

FTIR analysis

The FTIR analysis was done for different samples to predict the different bonds present in the samples, thereby predicting the compounds present. FTIR analysis was done for pure drug (plant extract), extracted sericin, alginate, sericin-alginate complex and drug loaded sericin-alginate hydrogel and the peaks were shown in (**Fig 12).**

The above graph represents the FTIR predicted spectra for the mentioned samples. Graph was plotted between wavenumber and transmittance (%). Based on the wavenumber, the functional group was predicted. In previous literature, the plant extract (drug) showed the characteristic peaks at 3800-3500 cm^{-1} (alcohol or polyphenols), 3000-3100 cm^{-1} (C-H of aldehyde), 1700-1600cm^{-1} (C=O bond), 1600-1500 cm^{-1} (C=C of alkene) and 1100-1000 (C-O of C-OH bond) [34]. Sericin showed the characteristic peaks at 1700-1600 cm^{-1} (C=O stretching amide I), 1600-1500 cm^{-1} (amide II) and 1500-1400 cm^{-1} (amide III C-N stretching coupled to N-H plane bending vibration)[40]. Sodium alginate showed the characteristic peaks at 3600-3000 cm^{-1} (stretching vibration of OH group), 2900-2840 cm^{-1} (C-CH vibration), 1600-1400 cm^{-1} (asymmetric/symmetric stretching vibration of COO^- groups) [41].

The extracted drug (plant extract) shows the peaks relatively similar to the literature like 3348 cm^{-1}, 1720 cm^{-1}, 1620 cm^{-1} 1512 cm^{-1}, 1087 cm^{-1} respectively. Sericin extracted from the silk cocoon shows the characteristic peak at 1627 cm^{-1}, 1527 cm^{-1} and 1404 cm^{-1} which are also similar to the literature. Alginate also shown the characteristic peak similar to the literature like 3379 cm^{-1}, 2931 cm^{-1}, 1604 cm^{-1} respectively. The spectrum of hydrogel shown peak at 393 and 347 cm^{-1} Peaks around 3000-3500 cm^{-1} in sericin, plant extract and alginate indicate the presence of the water molecules whereas such peaks were not found in the hydrogel which indicates that the water molecules got reduced during the hydrogel formation. Furthermore, the characteristic peaks of sericin appeared in the sericin-alginate complex and hydrogel indicates the presence of sericin.

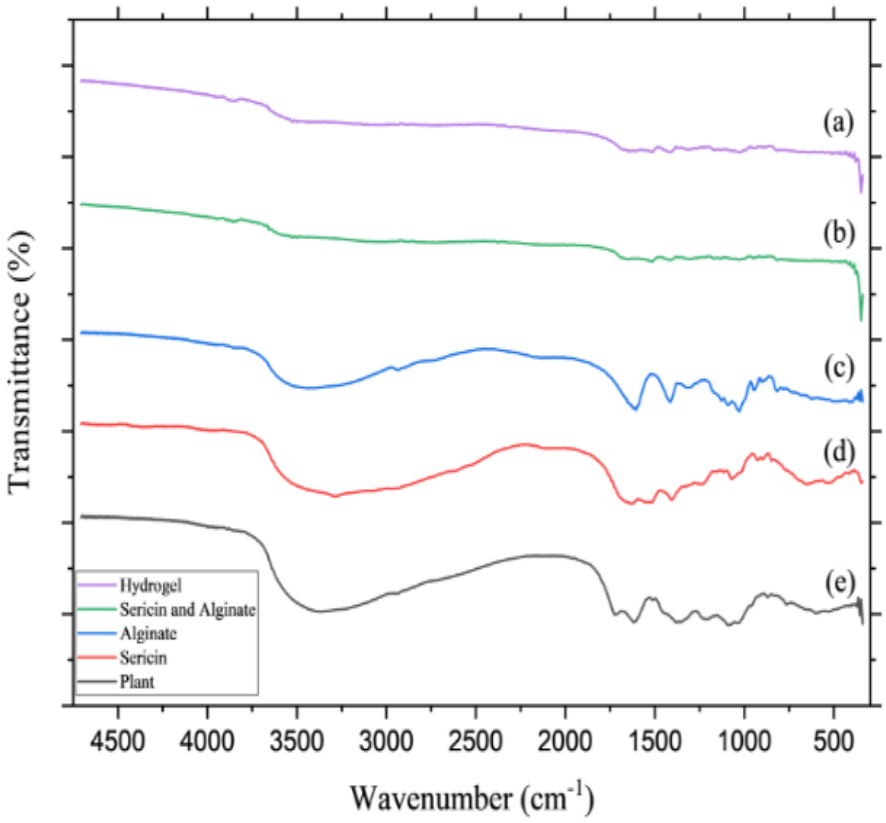

Fig. 12: FTIR spectra for a) Hydrogel b) Sericin-alginate complex c) Alginate d) Extracted sericin e) Drug (plant extract).

Properties of hydrogel

Water retention property

The water retention capacity was evaluated and presented in the **Fig. 13**. As time increases the water content present in the hydrogels get evaporated and the weight after time 't' gets reduced from the initial weight. The water retention % was rapidly decreases up to 180 mins and the water retention% reached to 31.42 %. From 180 min to 450 min the water retention% reduced to 19.71%. While continuing the experiment up to 840 min the further decrease in the water retention % was only about 4%. The results show that initially the rate of drying of the hydrogel is high due to removal of surface moisture content removal at this time period. However, latter period of time the reduction in the moisture removal is due to bounded moisture content [42].

Swelling behavior

Water is the major component of blood, such that hydrogels with good swelling property is best suitable to stop bleeding. Hydrogel with good swelling property has the ability to absorb higher volume of water. Here, the hydrogels fabricated had good swelling behavior. The percentage of swelling reached to 116.25 % on 12 hours of immersion in phosphate buffer at pH 7.4. The weight of the hydrogel gets doubled from the initial weight of the gel. On absorbing water, the hydrogel gets swollen, which is common and thus mimic living tissues with the same physical properties. [43] The swelling behavior was calculated and tabulated in **(Table 5).**

Water retention capacity of the fabricated hydrogel (10% sodium alginate-1.5% $Cacl_2$ loaded with aqueous plant extract) at different time intervals.

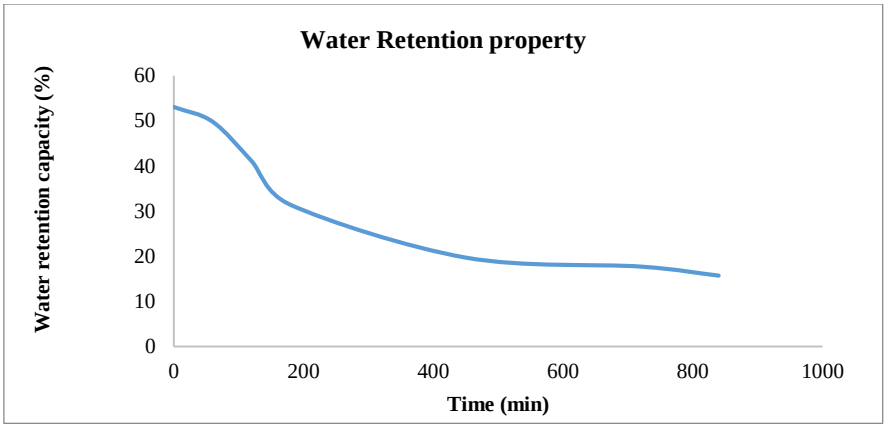

Fig. 13: Water retention property of the prepared hydrogel.

Table 5: Swelling behavior of the fabricated hydrogel (10% sodium alginate-1.5% $Cacl_2$ loaded with aqueous plant extract) at different time intervals.

Time (min)	Weight of hydrogel (g)	Swelling capacity (%)
0	1.6	0
10	1.88	17.5
20	2.22	38.75
30	2.39	49.4
90	2.45	53.12
150	2.69	68.13
210	2.87	79.4
270	2.98	86.25
390	3.13	95.6
510	3.29	105.63
600	3.39	111.9
720	3.46	116.25

Drug release kinetics

A standard calibration curve was plotted for different concentration of the aqueous plant extract of *S. leucopyrus* and absorbance at 530 nm as shown **in (Fig. 14 (a).** The plant extract released from the hydrogel was observed by measuring the absorbance of the phosphate buffer (pH 7.4) at 530 nm by varying the time interval and the results are presented in **Fig. 14 (b)**. The initial rate of release of extract is rapid up to 30 min and release% was reached to 16.7 3%. After that the gradual increase in release percentage continued to reach 37.6 % in 300 mins.

Antibacterial activity of hydrogels

The antibacterial activity of the fabricated hydrogels was evaluated against gram-positive bacterial strain and a gran-negative bacterial strain. **(Fig. 15)** and **(Table 6)** shows the zone of inhibition produced by hydrogel loaded with aqueous plant extract of *S. leucopyrus.* Similarly, the hydrogel loaded with CeONPs was tested for its antibacterial activity shown in **(Fig. 16)** and the zones of inhibition was tabulated **(Table 7).** However, the zone of inhibition results revealed that Gram-positive bacteria was susceptible to the hydrogels loaded with the plant extract and the CeONPs compared with the Gram-negative bacteria. Gram-negative bacteria did not show any effect towards the hydrogel loaded with aqueous plant extract of *S. leucopyrus* and the nanoparticles synthesized. Similarly, the hydrogels loaded with the aqueous plant extract of *S. leucopyrus* and the CeONPs synthesized using the aqueous plant extract did not show complete inhibitory activity but inhibition was observed. The number of colonies reduced as the incubation period increases. The zones of inhibition increased on increasing the incubation period which indicates the time dependent release of plant extract and CeONPs from synthesized hydrogel [44].

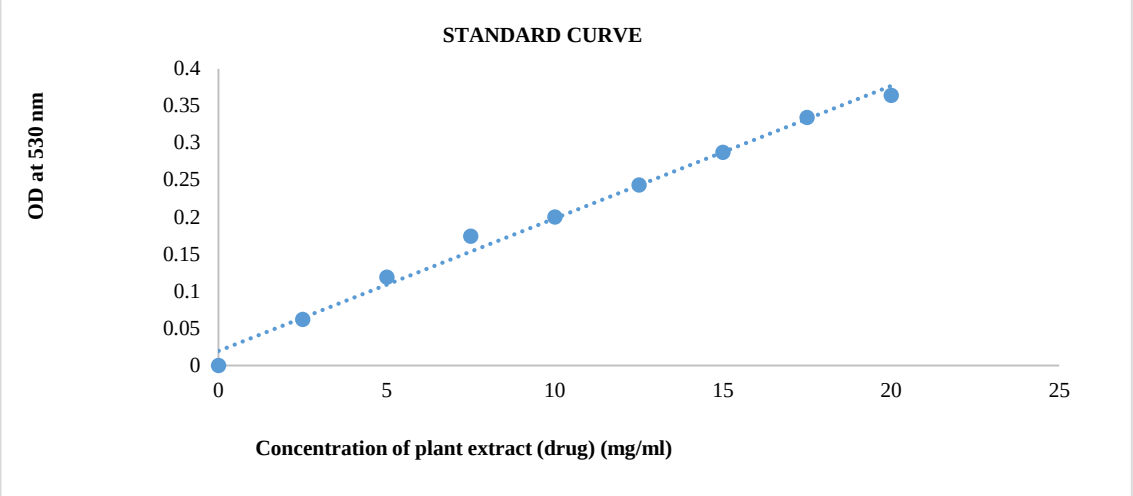

Fig. 14 (a): Standard calibration curve for the aqueous plant extract of *S. leucopyrus.*

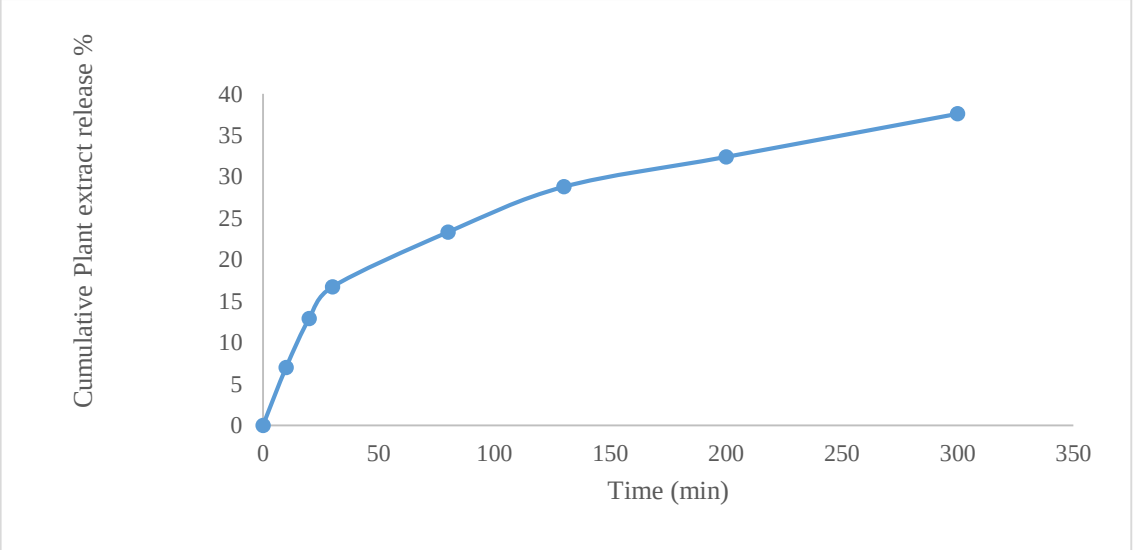

Fig. 14 (b): Plant Extract release from the hydrogel at different time intervals

Table 6: Antibacterial activity assays of hydrogel loaded with aqueous extract of *Securinega leucopyrus* using agar well diffusion method.

Name of the organism	Sample loaded	Incubation Time	Inhibition zones (mm)
Escherichia coli	Control (Amp^r)	24 hr	25
	Aqueous plant extract	24 hr	9
		48 hr	14
Staphylococcus aureus	Control (Amp^r)	24 hr	20
	Aqueous plant extract	24 hr	9
		48 hr	16

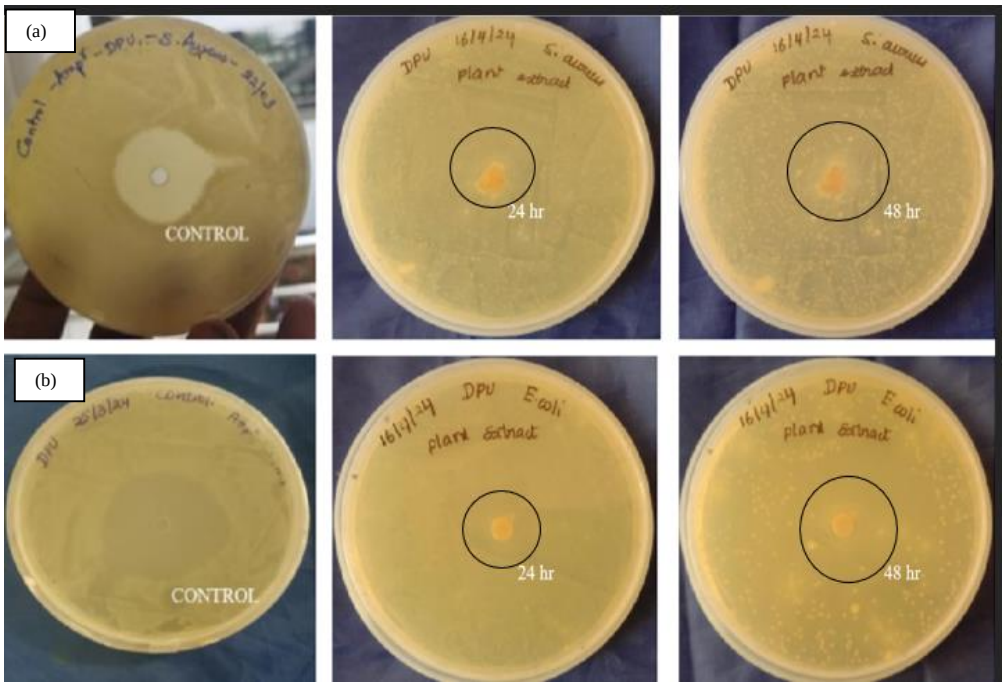

Fig. 15: Activity of hydrogel loaded with aqueous plant extract of *Securinega leucopyrus* depicting the zones of inhibition against the selected microorganisms, *Staphylococcus aureus* (a) and *Escherichia coli* (b).

Table 7: Antibacterial activity assays of hydrogel loaded with CeONPs using agar well diffusion method.

Name of the organism	Sample loaded	Incubation Time	Inhibition zones (mm)
Escherichia coli	Control (Amp^r)	24 hr	25
	Hydrogel with CeONPs	24 hr	7
		48 hr	9
Staphylococcus aureus	Control (Amp^r)	24 hr	20
	Hydrogel with CeONPs	24 hr	8
		48 hr	9

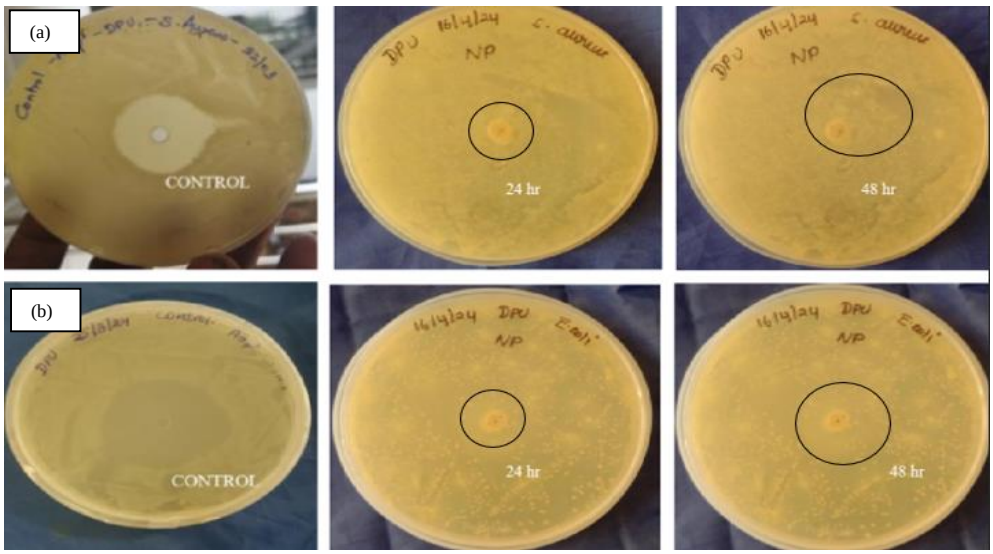

Fig. 16: Activity of hydrogel loaded with CeONPs depicting the zones of inhibition against the selected microorganisms, *Staphylococcus aureus* (a) and *Escherichia coli* (b).

Conclusions

In this study, CeONPs were synthesized through a green method such that the use of toxic compounds can be reduced. These nanoparticles were synthesized using *Securinega leucopyrus* extract, then sericin hydrogels containing the plant extract and the synthesized nanoparticles were successfully produced as a wound dressing for chronic diabetic wound healing applications. The plant extract also contains various bioactive compounds with tissue regeneration, cell proliferation, wound healing, antioxidant, antibacterial properties. Moreover, MMP-8 and MMP-9 serves as the potential target for healing wounds in diabetic patients such that, the interaction of the bioactive compounds present in the plant extract with these targets was studied and must be further investigated. The hydrogels were fabricated using different compounds such as sericin, extracted from silk cocoons and 10% sodium alginate with 1.5% calcium chloride as a cross-linker. Results showed that the plant extract and the nanoparticles exhibited antibacterial and antioxidant properties. Similarly, the hydrogel fabricated also showed antibacterial property with good water retention and swelling property. With these properties of the hydrogel fabricated could contribute towards wounds healing applications, majorly to chronic diabetic wounds.

Acknowledgements

We sincerely extend our heartfelt gratitude to Mepco Schlenk Engineering college, Sivakasi management for providing necessary facilities for completion of work.

REFERENCES

1. P. Saeedi, I. Petersohn, P. Salpea, B. Malanda, S. Karuranga, N. Unwin, S. Colagiuri, L. Guariguata, A.A. Motala, K. Ogurtsova, and J.E. Shaw, "Global and regional diabetes prevalence estimates for 2019 and projections for 2030 and 2045: Results from the International Diabetes Federation Diabetes Atlas", ***Diabetes Res Clin Prac***t, 157, 107843 (2019).
2. D. Cavan, J.D.R. Fernandez, Y. Huang and L. Makaroff, "IDF releases report of global survey on access to medicines and supplies for people with diabetes", ***Diabetes Res Clin Pract***, 129, 224–225 (2017).
3. P. E. H Schwarz, G. Gallein, D. Ebermann, A. Müller, A. Lindner, U. Rothe, I. T. Nebel and G. Müller, "Global Diabetes Survey: An annual report on quality of diabetes care", ***Diabetes Res Clin Pract***,100(1), 11–18 (2013).
4. A. P. Ugalde, G. R. Ordóñez, P. M. Quirós, X. S. Puente and C. López-Otín, "Metalloproteases and the degradome. In Matrix metalloproteinase protocols. Totowa", NJ: ***Humana Press*** 622, 3-29 (2010).
5. O.A. Peña, and P. Martin, "Cellular and molecular mechanisms of skin wound healing", ***Nat Rev Mol Cell Biol,*** 25(8), 1-18 (2024).
6. N. T. Bennett and G. S. Schultz, "Growth factors and wound healing: Biochemical properties of growth factors and their receptors", ***Am J Surg***, 165(6), 728–737 (1993).
7. A. Golchin, F. Shaikhnia, F. Heidari, D. Mahdi, Y. Hemmati and L. Tayebi, "Cell-derived materials for wound healing", Handbook of the Extracellular Matrix: Biologically-Derived Materials. Cham: Springer International Publishing, 1-22, (2023).
8. A. Gutierrez-Fernandez, M. Inada, M. Balbin, A. Fueyo, A. S. Pitiot, A. Astudillo, K. Hirose, M. Hirata, S.D. Shapiro, A. Noël, and Z. Werb, "Increased inflammation delays wound healing in mice deficient in collagenase-2 (MMP-8) ". FASEB J. 21(10), 2580–2591 (2007).
9. L.M. Bakshu, A.J. Ram, and R.V. Raju, Antimicrobial activity of *Securinega leucopyrus*. ***Fitoterapia***, 72(8), 930-933 (2001).
10. A. S. Ajmeer T. S. Dudhamal S. K. Gupta and V. Mahanta, "Katupila (*Securinega leucopyrus*) as a potential option for diabetic wound management", ***J Ayurveda Integr Med,*** 5, 60-63 (2014).
11. M.T. Khorasani, A. Joorabloo, H. Adeli, Z. Mansoori-Moghadam and A.

Moghaddam, "Design and optimization of process parameters of polyvinyl (alcohol)/chitosan/nano zinc oxide hydrogels as wound healing materials", ***Carbohydr Polym***, 207, 542-554 (2019).
12. A.S. Ahmed, U.K. Mandal, M. Taher, D. Susanti and J.M. Jaffri, "PVA-PEG physically cross-linked hydrogel film as a wound dressing: Experimental design and optimization", ***Pharm Dev Technol***, 23(8), 751-760 (2018).
13. A. Jahani-Javanmardi, M. Sirousazar, Y. Shaabani and F. Kheiri, "Egg white/poly (vinyl alcohol)/MMT nanocomposite hydrogels for wound dressing", ***J Biomater Sci Polym***, 27(12), 1262-1276 (2016).
14. A. Timofejeva, M. D'Este and D. Loca, "Calcium phosphate/polyvinyl alcohol composite hydrogels: A review on the freeze-thawing synthesis approach and applications in regenerative medicine", ***Eur Polym J,*** 95, 547-565 (2017).
15. K. Kalantari, A.M. Afifi, H. Jahangirian and T.J. Webster, "Biomedical applications of chitosan electrospun nanofibers as a green polymer–Review", ***Carbohydr Polym***, 207, 588-600 (2019).
16. W. Yang, E. Fortunati, F. Bertoglio, J. Owczarek, G. Bruni, M. Kozanecki, J. Kenny, L. Torre, L. Visai and D. Puglia, "Polyvinyl alcohol/chitosan hydrogels with enhanced antioxidant and antibacterial properties induced by lignin nanoparticles", ***Carbohydr Polym,*** 181, 275-284 (2018).
17. M. Saad, L.M. El-Samad, R.A. Gomaa, M. Augustyniak, and M.A. Hassan, "A comprehensive review of recent advances in silk sericin: Extraction approaches, structure, biochemical characterization, and biomedical applications", ***Int J Biol Macromol***, 250, 126067 (2023).
18. L. Lamboni, M. Gauthier, G. Yang, and Q. Wang, "Silk sericin: A versatile material for tissue engineering and drug delivery", ***Biotechnol Adv,*** 33(8), 1855-1867 (2015).
19. J. Wang, H. Liu, X. Shi, S. Qin, J. Liu, Q. Lv, J. Liu, Q.S. Li, Z. Wang and L. Wang, "Development and Application of an Advanced Biomedical Material-Silk Sericin", ***Adv Mater***, 36(23), 2311593 (2024).
20. T. You, Q. You, X. Feng, H. Li, B. Yi, and H. Xu, "A novel approach to wound healing: Green synthetic nano-zinc oxide embedded with sodium alginate and polyvinyl alcohol hydrogels for dressings" ***Int J Pharm***, 654, 123968 (2024).
21. Y. Rajesh, N.M. Khan, A.R. Shaikh, V.S. Mane, G. Daware, and G. Dabhade, "Investigation of geranium oil extraction performance by using soxhlet extraction", ***Mater Today: Proc***, 72, pp.2610-2617 (2023).
22. C. A. Lipinski "Lead- and drug-like compounds: the rule-of-five revolution", ***Drug Discov Today Technol,*** 1 (4), 337-341 (2004).
23. N. M. O'Boyle, M. Banck, C. A. James, C. Morley, T. Vandermeersch and G. R. Hutchison, "Open Babel: an open chemical toolbox", ***J Chem inf,*** 3(1),1–14 (2011).
24. M. G. Mamatha, M. A. Ansari, M. Y. Begum, D. Prasad B, A. Al Fatease, U. Hani, T. Ravikiran, "Green Synthesis of Cerium Oxide Nanoparticles, Characterization, and Their Neuroprotective Effect on Hydrogen Peroxide-Induced Oxidative Injury in Human Neuroblastoma (SH-SY5Y) Cell Line", ***ACS omega***, 9(2), 2639-2649 (2024).
25. L.K. Rocha, L.I. Favaro, A.C. Rios, E.C. Silva, W.F. Silva, T.P. Stigliani, M. Guilger, R. Lima, J.M. Oliveira Jr, N. Aranha, and M.Tubino, "Sericin from Bombyx mori cocoons. Part I: Extraction and physicochemical-biological characterization for biopharmaceutical applications", ***Process Biochem***, 61, 163-177 (2017).
26. M. M. Bradford, "A rapid and sensitive method for the quantitation of microgram quantities of protein utilizing the principle of protein-dye binding", ***Analyt Biochem***, 72, 248–254 (1976).

27. R. Bascou, J. Hardouin, M.A.B. Mlouka, E. Guénin, and A. Nesterenko, "Detailed investigation on new chemical-free methods for silk sericin extraction", ***Mater Today Commun***, 33, 104491 (2022).
28. M. Li, Y. Dong, M. Wang, X. Lu, X. Li, J. Yu, and B. Ding, "Hydrogel/nanofibrous membrane composites with enhanced water retention, stretchability and self-healing capability for wound healing", ***Compos B Eng***, 257,110672 (2023).
29. S. Baptista-Silva, S. Borges, A.R. Costa-Pinto, R. Costa, M. Amorim, J.R. Dias, O. Ramos, P. Alves, P.L. Granja, R. Soares and M. Pintado, "In situ forming silk sericin-based hydrogel: A novel wound healing biomaterial", ***ACS Biomater Sci Eng***, 7(4), 1573-1586 (2021).
30. K. Sriram, P. Uma Maheswari, K.M. Meera Sheriffa Begum, and G. Arthanareeswaran, "Functionalized chitosan with super paramagnetic hybrid nanocarrier for targeted drug delivery of curcumin", ***Iran Polym. J***, 27, 469-482 (2018).
31. B. Farasati Far, M.R. Naimi-Jamal, M. Jahanbakhshi, A. Hadizadeh, S. Dehghan, and S. Hadizadeh, "Enhanced antibacterial activity of porous chitosan-based hydrogels crosslinked with gelatin and metal ions", ***Sci Rep***, 14(1), 7505 (2024).
32. R. Yuvarajan, D. Natarajan, C. Ragavendran, and R. Jayavel, "Photoscopic characterization of green synthesized silver nanoparticles from Trichosanthes tricuspidata and its antibacterial potential", ***J Photochem Photobiol B***, 149, 300-307 (2015).
33. C. Sarkar, M. Mondal, K. Al-Khafaji, D.M. El-Kersh, S. Jamaddar, P. Ray, U.K. Roy, M. Afroze, M. Moniruzzaman, M. Khan, and U.H. Asha, "GC–MS analysis, and evaluation of protective effect of Piper chaba stem bark against paracetamol-induced liver damage in Sprague-Dawley rats: Possible defensive mechanism by targeting CYP2E1 enzyme through in silico study", ***Life Sci***, 309, 121044 (2022).
34. K. Rajoriya, A. Singhal, R. Meena, and A. Kumari, "Biogenic Synthesis and Characterisation of *Flueggea leucopyrus* Willd Leaf Mediated Copper Nanoparticles for Antibacterial, Antioxidant, and Antidiabetic Activities", ***J Herb Med***, 44, 100859 (2024).
35. A. Chinnathambi, S.A. Alharbi, D. Joshi, V. Saranya, G.K. Jhanani, R. On-Uma, K. Jutamas, and W. Anupong, "Synthesis of AgNPs from leaf extract of Naringi crenulata and evaluation of its antibacterial activity against multidrug resistant bacteria", ***Environ Res***, 216(part 1), 114455 (2023).
36. S. Parvathy, G. Manjula, R. Balachandar and R. Subbaiya, "Green synthesis and characterization of cerium oxide nanoparticles from Artabotrys hexapetalus leaf extract and its antibacterial and anticancer properties", ***Mater Lett***, 314, 131811 (2022).
37. M. Summer, S. Ali, H.M. Tahir, R. Abaidullah, H. Tahir, S. Mumtaz, S. Mumtaz, S.A. Butt, and M. Tariq, "Silk Sericin Protein: Turning Discarded Biopolymer into Ecofriendly and Valuable Reducing, Capping, and Stabilizing Agent for Nanoparticles Synthesis Using Sonication", ***Macromol Chem Phys***, 224(17), 2300124 (2023).
38. P. Aramwit, S. Damrongsakkul, S. Kanokpanont, and T. Srichana, "Properties and antityrosinase activity of sericin from various extraction methods", ***Biotechnol Appl Bioc***, 55(2), 91-98 (2010).
39. H. Teramoto and M. Miyazawa, "Molecular orientation behavior of silk sericin film as revealed by ATR infrared spectroscopy", ***Biomacromolecules,*** 6(4), 2049–2057 (2005).
40. Y. Zhang, X. Cao, J. Zhang, G. Zhang, M. Zhu, H. Yan and Y. Li, "A novel injectable sericin hydrogel with strong

fluorescence for tracing", ***Int J Biol Macromol***, 258(Pt 2), 129000 (2024).
41. M. Paswan, A.K.S.Chandel, N.I. Malek, and B.Z. Dholakiya, "Preparation of sodium alginate/Cur-PLA hydrogel beads for curcumin encapsulation", ***Int J Biol Macromol***, 254(Pt 3), 128005 (2024).
42. G. Chhetry, and P.S.G. Pattader, "Effect of patterns on Polyacrylamide hydrogel surface towards enhancement of water retention", ***Polymer***, 127362 (2024).
43. T. Wu, H. Liu, H. Wang, Y. Bu, J. Liu, X. Chen, H. Yan, and Q. Lin, "Fabrication of alginate/sericin/cellulose nanocrystals interpenetrating network composite hydrogels with enhanced physicochemical properties and biological activity", ***J Appl Polym Sci***, 141(10), e55052 (2024).
44. T. Pourseif, R. Ghafelehbashi, M. Abdihaji, N. Radan, E. Kaffash, M. Heydari, M. Naseroleslami, N. Mousavi-Niri, I. Akbarzadeh, and Q. Ren, "Chitosan-based nanoniosome for potential wound healing applications: Synergy of controlled drug release and antibacterial activity", ***Int J Biol Macromol***, 230, 123185 (2023).

Bull. Pharm. Sci., Assiut University, Vol. 47, Issue 2, 2024, pp. 699-721

نشرة العلوم الصيدلية
جامعة أسيوط

BULL. PHARM. SCI. Assiut Univ.

تطوير هيدروجيل السيريسين المدمج مع جزيئات أكسيد السيريوم المتناهية الصغر المحضرة بالكيمياءالخضراء باستخدام Securine galeucopyrus للإستعمال فى شفاء الجروح المزمنة الناتجة عن مرض السكري

ك. سريرام* – ج. بريانكا – تينيسي. دهانوشري – أ. أودهايادارشيني

قسم التكنولوجيا الحيوية ، كلية الهندسة ميبكو شلينك ، سيفاكاسي – ٦٢٦٠٠٥، تاميل نادو ، الهند

أثارت المواد الحيوية المصنوعة من السيريسين من نفايات شرنقة Bombyx mori في الوقت الحاضر اهتمامًا متزايدًا بين الأبحاث العلمية نظرًا لتوافقها الحيوي العالي مع مجموعة واسعة من الخلايا. و تم في هذه الدراسة ، تحضير جسيمات أكسيد السيريوم المتناهية الصغر (CeONPs) من المستخلص النباتي لـ Securinegaleucopyrus وتم تحميلها علي هيدروجيل السيريسين لتطوير مركب جديد متناهى الصغر يستعمل فى إلتئام الجروح. وتم إستعمال المستخلص النباتي كعامل اختزال ومثبت يساعد في تحويل نترات السيريوم إلى أكسيد السيريوم .

وتم تحليل خصائص الجسيمات المتناهية الصغر المحضرة فيزيائيا وكيميائيا بواسطة القياس الطيفي المرئي للأشعة فوق البنفسجيةUV))، وتشتت الضوء الديناميكي (DLS)، والفحص المجهرى الإلكتروني الماسح (SEM)، والنافذ (TEM). وأظهر الطيف المرئي للأشعة فوق البنفسجية للجسيمات النانوية المركبة ذروة مميزة عند ٢٤٠ نانومتر. وتم فحص حجم وشحنة الجسيمات المتناهية الصغر باستخدام DLS ووجد أنها ١٨٦,٧ نانومتر و–٢٢,٥ مللي فولت. وأثبتت النتائج أن المستخلص النباتي والجسيمات المتناهية الصغر لأكسيد السيريوم له نشاطًا مضادًا للبكتيريا ضد الكائنات الحية الدقيقة إيجابية الجرام (المكورات العنقودية الذهبية) وسالبة الجرام. وكذلك نشاطًا مضادًا للأكسدة بنسبة ٨٣,٤% و٧٦,٤٨% على التوالي. وقد أظهر الهيدروجيل خاصية جيدة لاحتجاز الماء وسلوك التورم. وتمت دراسة حركية إنطلاق الدواء للحصول على السيريسين هيدروجيل . وأظهر المستخلص النباتي والهيدروجيلات المحملة بـ CeONPs أيضًا نشاطًا جيدًا مضادًا للبكتيريا ، و توصلت النتائج إلى أن هيدروجيل السيريسين النانوي يمكن أن يكون صياغة واعدة ومحتملة لشفاء الجروح المزمنة.